Available online at www.sciencedirect.com
ScienceDirect
Journal of the European Ceramic Society 27 (2007) 1559–1564
www.elsevier.com/locate/jeurceramsoc

Micromechanical properties of a hydroxyapatite/poly-L-lactide biocomposite using nanoindentation and modulus mapping

P.S. Uskokovic [a,*], C.Y. Tang [b], C.P. Tsui [b], N. Ignjatovic [c], D.P. Uskokovic [c]

[a] *Faculty of Technology and Metallurgy, University of Belgrade, Karnegijeva 4, 11000 Belgrade, Serbia and Montenegro*
[b] *Department of Industrial and Systems Engineering, The Hong Kong Polytechnic University, Hung Hom, Kowloon, Hong Kong, PR China*
[c] *Institute of Technical Sciences of the Serbian Academy of Sciences and Arts, Knez Mihailova 35/IV, 11000 Belgrade, Serbia and Montenegro*

Available online 5 June 2006

Abstract

Biocomposites with ceramic fillers and polymer matrix are becoming attractive materials for bone tissue replacements. Nanoindentation has been used to locally characterize the surface mechanical properties of the hydroxyapatite/poly-L-lactide (HAp/PLLA) biocomposite. Additionally, differences in the mechanical properties of HAp phase were successfully characterized as a function of surface morphology by using a high-resolution modulus mapping technique. HAp granules consist of agglomerates of grainy clusters. Mechanical properties of ceramic grains and PLLA are in fair agreement with literature data. High-resolution methods were able to measure the properties of boundary phases between grains and the pore regions between particles in the agglomerate. After short-time immersion in distilled water, material surface showed a large decrease in storage modulus.

Keywords: Composites; Mechanical properties; Biomedical applications; Nanoindentation

1. Introduction

Composites with ceramic phase such as hydroxyapatite (HAp) and bioresorbable polymer phase such as poly-L-lactide (PLLA) have advantages over the conventional tissue replacement materials in that their mechanical and biological properties can be tailored in order to meet specific clinical requirements.[1–4] During composite processing, residual micropores in the ceramic phase and degradation of the polymer due to the thermal treatment, lead to constituent material properties that could be severely different from the bulk ones. Balac et al.[5] reported that the elastic modulus of the HAp/PLLA composite unit cell model predictions were as much as 50% less than the reported literature values for hot compacted samples due to the overestimation of the ceramic and polymer input material properties. A method is therefore needed to determine the properties of each phase separately, leading to information that is valuable for the development of new materials and for modeling purposes. Besides in a number of materials such as thin films and hard coatings, characterization of mechanical properties in fine spatial resolutions is becoming increasingly important in polymers or polymer blends,[6,7] fine grained ceramics,[8] phase-separated materials and composites.[9–12] Nanoindentation method is recently applied to a range of biomaterials such as ultra-high-molecular-weight polyethylene, sintered bioceramic powders and functionally graded bioactive composites.[13,14]

Polymer biocomposites are phase-separated both in bulk and on surface. The hardness and modulus on macroscopic scales of biocomposites are important properties for practical applications. However, to the best of our knowledge, there is no report that investigates the microscopic mechanical properties in the different phases of biocomposites, especially across the interface. These microscopic properties on the surface of composites are useful for understanding the surface details of a product and the components' contribution to the overall surface properties of composites. In this study, the elastic modulus and hardness of HAp/PLLA composite on micro-scales are evaluated using nanoindentation technique with addition of modulus mapping

* Corresponding author. Tel.: +381 11 3303659; fax: +381 11 3370387.
E-mail address: puskokovic@tmf.bg.ac.yu (P.S. Uskokovic).

0955-2219/$ – see front matter © 2006 Elsevier Ltd. All rights reserved.
doi:10.1016/j.jeurceramsoc.2006.04.122

technique of the ceramic granules, which comprise pure ceramic, boundary between grains and surface pores.

2. Experimental procedure

2.1. Sample preparation

Calcium hydroxyapatite (HAp) was obtained by precipitation from calcium nitrate and ammonium phosphate solutions in an alkaline medium.[4] The resulting gel was granulated at room temperature. HAp granules were calcined at 1100 °C for 6 h, and granules of 200–500 μm in size were used in our experiments. Commercial poly-L-lactide (Fluka, Germany) of molecular weight of 100,000 g/mol was used as a polymer component. In all samples, HAp/PLLA mass ratio was 80:20. The composite powder was poured into rectangular mould (40 mm × 12 mm × 3 mm) and was compacted by hot pressing (a CARVER press Inc. Auto C 3889) at temperature of 165 °C and pressure of 5 t for 7 min. The specimens were carefully cut from the composite blocks, polished initially with a series of grit papers and then on polishing cloths with different diamond suspensions down to 0.1 μm.

2.2. Nanoindentation and modulus mapping techniques

Nanoindentation and modulus mapping experiments were performed with a TriboScope Nanomechanical Testing System (Hysitron, Minneapolis, MN) equipped with in situ imaging mode. The nanoindentation instrument consists of a force displacement transducer with electrostatic force actuation and displacement sensing electronics. During indentation, a diamond indenter is pushed into the surface of the sample while the load and displacement of the indenter are continuously monitored with resolutions of 0.1 μN and 0.2 nm, respectively. A Berkovich indenter was used, which is a three-sided pyramid with a total included angle of 142.3° and a tip radius, which is determined to be 150 nm by standard nanoindentation protocol. Using a very light loading force (0–1 μN), the in situ imaging method can measure surface topography without causing any damage to the surface. Subsequently, heavier loading forces with a wide range of values (0–2 mN) can be applied to the tip, so that nanoindentation hardness tests under various loading conditions can be conducted. In the nanoindenter, an optical microscope was used to observe the surface morphology and place the indents on desired locations.

From the load–depth penetration curves (Fig. 1), the elastic modulus and hardness are calculated based on the methods proposed by Oliver and Pharr[15]:

$$E_r = \frac{\sqrt{\pi}S}{2\sqrt{A}} \quad (1)$$

where S is the slope of the initial portion of the unloading curve, A is the indenter contact area, and E_r, the reduced modulus, is defined by:

$$\frac{1}{E_r} = \frac{1-\upsilon_m^2}{E_m} + \frac{1-\upsilon_i^2}{E_i} \quad (2)$$

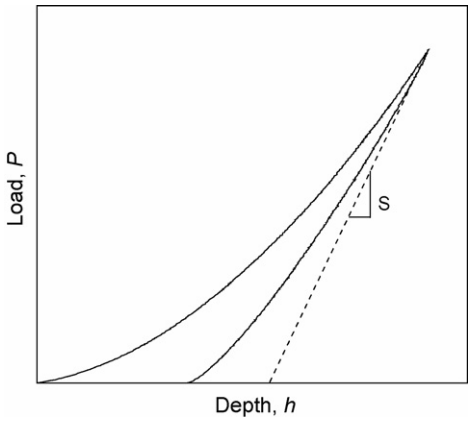

Fig. 1. Typical load–penetration depth curve obtained from a nanoindentation test on a fused silica.

where E_m and υ_m are the Young's modulus and Poisson's ratio of the indented materials, respectively, and E_i and υ_i are those of the diamond indenter, given as $E_i = 1141$ GPa and $\upsilon_i = 0.07$. For the curve presented in Fig. 1 the reduced modulus and hardness values were 69.83 and 9.89 GPa, respectively.

Quantitative modulus maps in the form of SPM (scanning probe microscopy) images were acquired using the direct force modulation (nanoDMAs) operating mode of a TriboScope nanoindenter. The advantage of force modulation is that the contact stiffness can be directly obtained continuously during indentation, thus forming a modulus mapping, which could be an ideal technique for multiphase and composite materials. In force modulation, a quasi-static force (dc force) was superimposed by a 1 μN sinusoidal force (ac force) with a frequency of 200 Hz. A lock-in amplifier was utilized to analyze the sample response, yielding displacement amplitude and the phase shift between the ac force and the displacement. The contact stiffness and material damping were calculated from the amplitude and phase shift using a dynamic model. A review of quantitative modulus mapping implementation details can be found in work of Asif et al.[16,17] and Balooch et al.[18]

3. Results and discussion

3.1. Nanoindentation testing

Three sets of quasi-static indents on different regions aimed to cover ceramic phase and surrounding polymer phase are presented in this study. In the first test set, during first 5 s indenter was driven into the sample with a 200 μN/s loading rate. After reaching the maximum load of 1000 μN, the indenter was held for 2 s in order to reduce the creeping effect before unloading at a rate of 200 μN/s. The distance between indents on HAp and PLLA was set to be 1.5 and 3 μm, respectively, in order to avoid possible overlapping of plastic deformation zone onto neighbouring indents. In order to achieve more precise profile, in the second line of indents the spacing was varied between 1 and 3 μm and accordingly the load was changed from 1000 (pure ceramic phase) to 50 μN (pure matrix phase). For the third set of

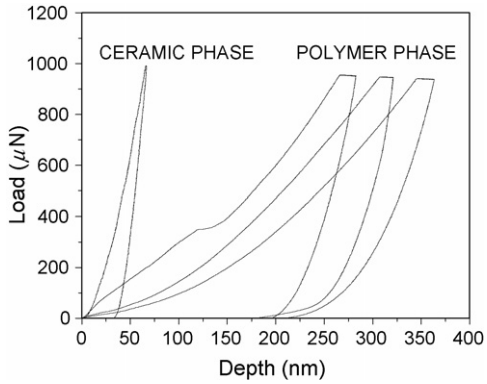

Fig. 2. Characteristic load–depth curves for indents on ceramic and various parts of matrix phase.

indents, loading rate and indent spacing were set to 40 μN/s and 0.7–1 μm, respectively, and loading was maintained constant on the value of 200 μN. Olek et al.[19] reported that hardness of PMMA is not affected by the load/unload rate and modulus does not exhibit significant changes with increasing rates above 30 μN/s.

Fig. 2 shows typical loading and unloading curves during indentations on the surfaces of HAp and PLLA phases for the first line of indents. The load controlled indentation clearly indicated that the displacement on the pure matrix phase was higher than that on ceramic phase. Pop-in marks observed in the polymer near the ceramic are a consequence of deformation field influence between two phases. For the ceramic phase, no pop-in marks appear during loading. Effects such as proximity of reinforcing phase and creep at holding load could influence measured values and additional studies may help to derive result adjustment in order to make nanoindentation more precise for investigation of various types of materials.[20,21] In this issue, we have focused on the change in the modulus and hardness, rather than on their absolute values.

Lines of elastic modulus and hardness are shown in Fig. 3. In order to estimate the Young's modulus of a specimen, the value of Poisson's ratio is needed. In the present study, the Young's modulus was calculated by assuming the Poisson's ratio of 0.28 and 0.45 for HAp and PLLA, respectively.

Results presented in Fig. 3(a) and (b) clearly reveal the gradient distribution near the interface. Surprisingly, by observing Fig. 3(c), the median values belong to the ceramic region, even though relatively low indent loads are imposed in order to prevent particle edges from sinking in the matrix. HAp granules consist of agglomerates of grainy clusters. Modulus and hardness decrease varies in the ceramic phase in dependence of the indent point location, which could be pure ceramic or the particle edge and the polymer and void regions between particles in the agglomerate. Fig. 3(c) shows matrix hardening in the vicinity of the HAp probably due to the influence of deformation fields of the ceramic and polymer phase. Mechanical testing of transition region measures the properties, which have resulted from combined factors indicating the need of using ultra low load values and smaller spacing between the

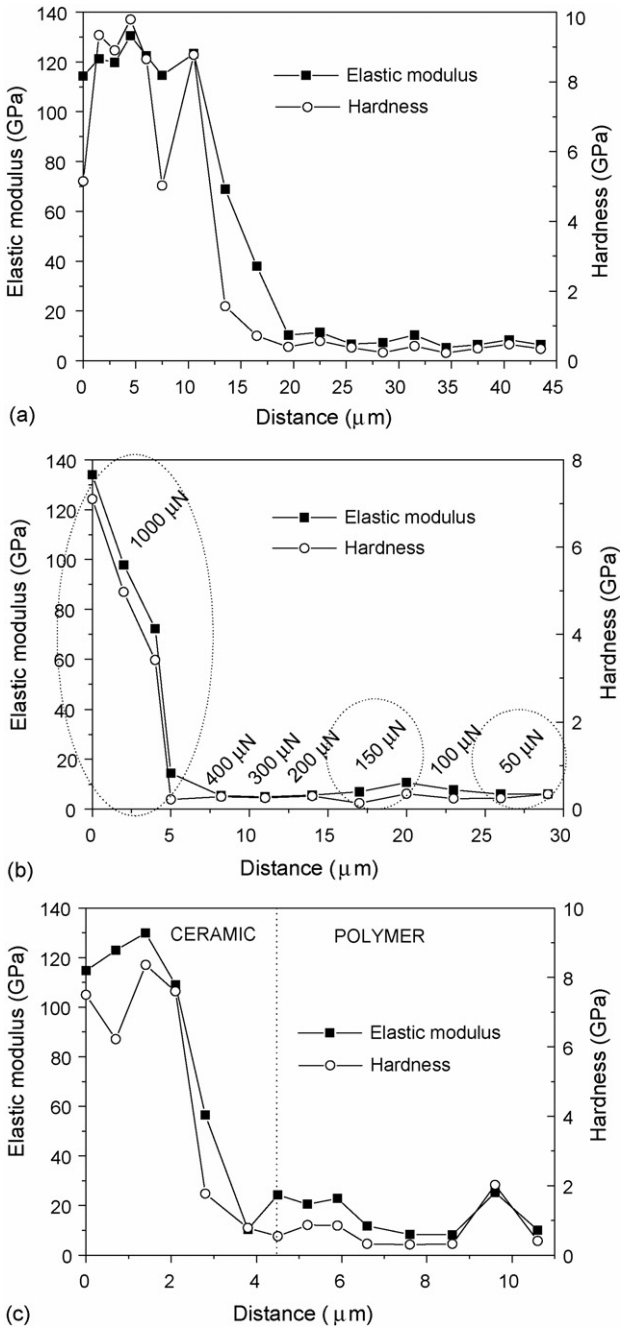

Fig. 3. Elastic modulus and hardness vs. position: (a) constant load 1000 μN; distance between indents 3 μm; (b) various loads; distance between indents from 1 to 3 μm; (c) constant load 200 μN; distance between indents from 0.7 to 1 μm.

indents, which will be addressed in the second part of this study.

The HAp average elastic modulus was 120.90 and 119.30 GPa for applied indentation loads of 1000 and 200 μN, respectively. The indents near the interface with matrix were excluded from calculations. The measured values for these materials were comparable to the upper bound of the HAp bulk values.[22] The average values for hardness was found to be 7.95 and 7.42 GPa.

The magnitude of the elastic modulus of PLLA matrix was found to be 8.10 and 6.68 GPa. Accordingly, measured average

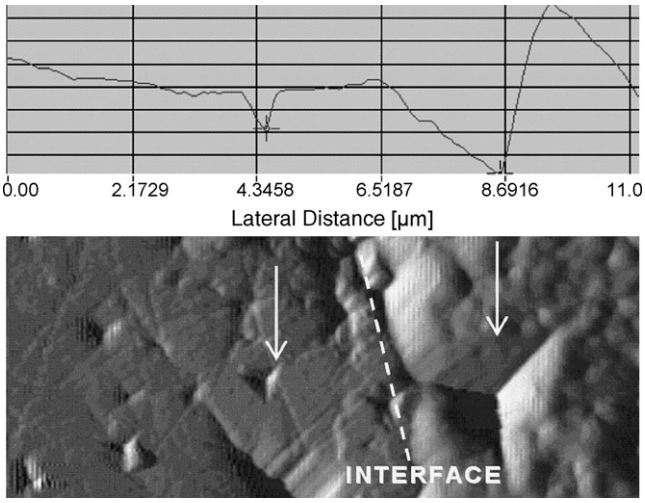

Fig. 4. In situ imaging scans of the indents near the ceramic/polymer interface with surface profile.

hardness values were 0.378 and 0.272 GPa. However, the average modulus of the PLLA is higher than was expected based on the literature data for the modulus in compression (4.8 GPa), bending (6.5 GPa)[23] and nanoindentation.[24] This could be due to the influence of HAp phase underneath the indentation site because of a high HAp content and relatively large indentation depths. Separately, we can conclude that the test with imposed indent load of 200 μN yielded higher results for PLLA because the polymer was probed in the vicinity of the ceramic. The influence of the ceramic phase was shown to be more detrimental to the polymer properties than the indent load. In comparison to bending modulus, the nanoindentation tend to derive higher results because the sample locations free from imperfections are selected for testing by in situ imaging. The bend test determines the modulus on the bulk level, and will incorporate flaws in the interior of the specimen. The two methods also induce a different stress state in the material, which could also lead to differences in the measured moduli.[24]

In situ imaging scans of the indents near the ceramic/polymer interface with surface profile are presented in Fig. 4. Presented scan belongs to indents presented on Fig. 3(c) showing that there is no pile-up around the HAp indent while around PLLA indent, pile-up is formed at the opposite part of the ceramic phase location.

For composites consisting of materials with large difference in mechanical properties, such as the HAp/PLLA, the softer material dictates the minimum separation of indents. This can be

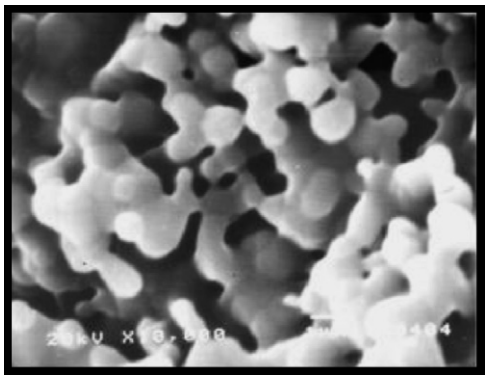

Fig. 5. SEM of the HAp granule surface, which shows the grain agglomeration.

observed in Fig. 4, as the indentations in the ceramic region are far apart, while in the polymer, the indent causes large imprint, causing concerns about the accuracy of the measurements. By using more refined measurement such as modulus mapping, the material under the tip is probed within the elastic region, and therefore, once the tip force is removed, the material returns to its original shape with no local residual stress or permanent deformation.

3.2. Modulus mapping

The microstructure of the ceramic phase obtained by SEM is presented in Fig. 5. HAp particles are arranged in rounded grainy clusters, which continuously grow and become bonded into agglomerates. These mutually bonded agglomerates, with voids 0.1–3 μm in diameter between them, form the basis of the HAp structure. These voids represent the inner porosity of the HAp phase. Porosity of the HAp surface enables penetration of potentially existing liquid phase into its structure. Non-compact granules are viable for biomedical applications since they enable adhesion between osteoclasts and osteoblasts after embedding in the tissue. In order to characterize HAp surface, quantitative modulus maps were obtained by using the direct force modulation (nanoDMA) operating mode of a TriboScope nanoindenter. Fig. 6 presents a map of an area of 5 μm × 5 μm obtained by in situ imaging in contact mode, which contains a selected region of the HAp particle. This figure reveals topographical, amplitude, phase and gradient shift. Knowing these phase differences and amplitude variations of modulation, along with the spring constant and damping coefficient of the transducer, the storage and loss moduli of the area were calcu-

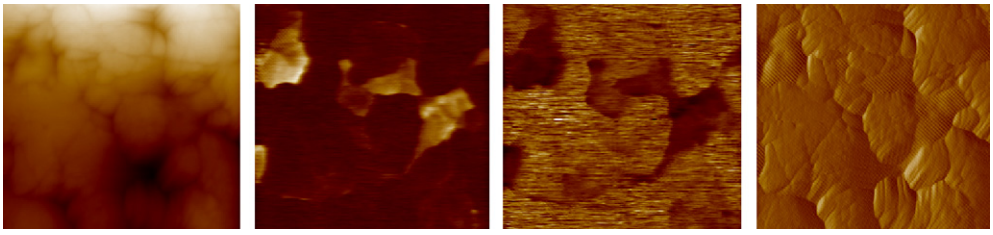

Fig. 6. Phase images obtained by in situ imaging (topographical, amplitude, phase and gradient shift).

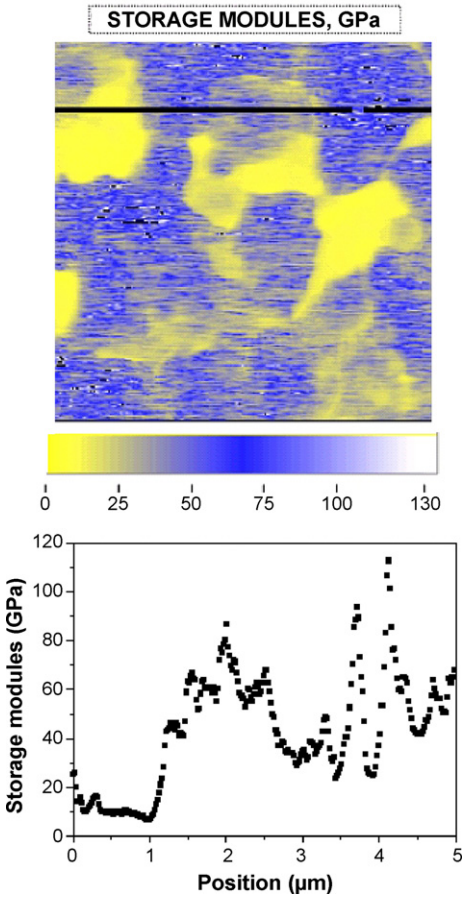

Fig. 7. Storage modulus map with the line scan of the HAp surface.

lated and the storage moduli were displayed as an image with a selected line scan in Fig. 7. The loss components of HAp were relatively small compared to storage components, suggesting that the storage modulus was practically equal to that of the elastic modulus. Significant local variations at the particle surface, which comprise pure ceramic, boundary regions between grains and surface pores filled with PLLA, could be observed from the map and the cross-sections drawn across the ceramic phase.

Additionally, preliminary tests were performed with samples, which were immersed in distilled water at 37 °C for 48 h. Average storage modulus frequency histograms for four different positions for virgin and immersed sample are shown in Fig. 8(a) and (b), respectively. It is easy to observe that the storage modulus significantly decreased after immersion. This is in agreement with experimental observations claiming that due to the penetration of water molecules, the PLLA is swelling after first period of immersion, in that way covering pure ceramic regions of the particle.[25]

Dissolution of composite phases was not expected because of the experimental conditions set for this study. Additional explanation for the reduction in storage modulus is attributed to the fact that interfaces between HAp and polymer phase allows water uptake thus reducing their mechanical properties. As the HAp–PLLA contact area is large bearing in mind the content and the granule-like structure of HAp, the degree of storage modulus was reasonably remarkable in present study. For neat polymer and composites with lower HAp fraction, the uptake of fluid molecules tends to ease the mobility of polymer chains, leading to an increase in susceptibility to deformation.[26] Zhang and Ma[27] reported that the molecular weight decrease within smaller time frame was not large enough to cause mechanical property deterioration of PLLA, presumably due to the slow hydrolysis rate of the hydrophobic PLLA. This study revealed that almost no apatite microparticles were observed on the surfaces of the PLLA pore walls after 3 days of incubation. Wright-Charlesworth et al.[24] reported a modulus decrease of ∼4.5% for PLLA after 4 weeks of in vitro conditioning time in 37 °C PBS. By using nanoindentation, it might be possible to determine changes in mechanical properties sooner than with traditional tests and the insight into the mechanical property gradients over small areas could yield information about the molecular level degradation.[24]

In conventional nanoindentation, the residual imprint on virgin surface could not be repeated at the same location because the surface is damaged due to larger force. Since the effect of immersion in water or simulated body fluids can be studied effectively if the indents are probed at the same position after repeatedly immersing the sample, small forces during nanoDMA test provide conditions that could lead to conclusions useful for describing surface-mechanical and biological features of the artificial implant materials.

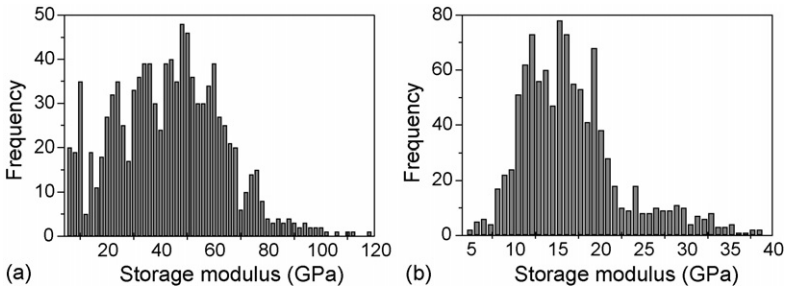

Fig. 8. Results obtained from nanoDMA by testing four different positions on the HAp granule. Storage modulus frequency histogram for: (a) non-immersed; (b) immersed sample.

4. Conclusions

Profiles of the local hardness and modulus obtained from the lines of indents on ceramic and polymer phases were successfully made on the surface of HAp/PLLA biocomposite. Elastic modulus and hardness of the polymer and ceramic phase are in fair agreement with experimental data. A larger variation of data is observed in the regions near the polymer/particle interface, in particular in the outer region of particles.

The new modulus mapping method allowed quantitative determinations with high spatial resolution of storage and loss moduli variations at the surface of ceramic granules, which comprise pure ceramic, boundary between grains and surface pores. After short-time immersion in distilled water, material surface showed a large decrease in storage modulus.

Acknowledgements

The authors wish to acknowledge the financial support from the Research Committee of The Hong Kong Polytechnic University (Project codes: G-YD67 and G-YX34) and the Ministry of Science and Environmental Protection, Republic of Serbia. In addition, the authors would like to thank Dr. Vincent Y.F. Li from the Design and Manufacturing Services Facility of The Hong Kong University of Science and Technology for providing us with the equipment and William C.C. Wong and Peter L.K. Chun for their assistance in nanomechanical tests.

References

1. Verheyen, C. C. P. M., de Wijn, J. R., van Blitterswijk, C. A. and de Groot, K., Evaluation of hydroxyapatite/poly(L-lactide) composites: mechanical behaviour. *J. Biomed. Mater. Res.*, 1992, **26**, 1277–1296.
2. Suchanek, W. and Yoshimura, M., Processing and properties of hydroxyapatite-based biomaterials for use as hard tissue replacement implants. *J. Mater. Res.*, 1998, **13**, 94–117.
3. Hench, L., Bioceramics. *J. Am. Ceram. Soc.*, 1998, **81**, 1705–1728.
4. Ignjatovic, N., Tomic, S., Dakic, M., Miljkovic, M., Plavsic, M. and Uskokovic, D., Synthesis and properties of hydroxyapatite/poly-L-lactide composite biomaterials. *Biomaterials*, 1999, **20**, 809–816.
5. Balac, I., Uskokovic, P. S., Aleksic, R. and Uskokovic, D., Predictive modeling of the mechanical properties of particulate hydroxyapatite reinforced polymer composites. *J. Biomed. Mater. Res.*, 2002, **63**, 793–799.
6. Klapperich, C., Komvopoulos, K. and Pruitt, L., Nanomechanical properties of polymers determined from nanoindentation experiments. *ASME J. Tribol.*, 2001, **123**, 624–631.
7. Zhu, S. H., Chan, C. M. and Mai, Y. W., Micromechanical properties on the surface of PVC/SBR blends spatially resolved by a nanoindentation technique. *Polym. Eng. Sci.*, 2004, **44**, 609–614.
8. Gong, J., Peng, Z. and Miao, H., Analysis of the nanoindentation load–displacement curves measured on high-purity fine-grained alumina. *J. Eur. Ceram. Soc.*, 2005, **25**, 649–654.
9. Furnemont, Q., Kempf, M., Jacques, P. J., Goken, M. and Delannay, F., On the measurement of the nanohardness of the constitutive phases of TRIP-assisted multiphase steels. *Mater. Sci. Eng. A*, 2002, **328**, 26–32.
10. Torralba, J. M., Velasco, F., Costa, C. E., Vergara, I. and Caceres, D., Mechanical behaviour of the interphase between matrix and reinforcement of Al 2014 matrix composites reinforced with $(Ni_3Al)_p$. *Composites A*, 2002, **33**, 427–434.
11. Campo, M., Urena, A. and Rams, J., Effect of silica coatings on interfacial mechanical properties in aluminium–SiC composites characterized by nanoindentation. *Scripta Mater.*, 2005, **52**, 977–982.
12. Engqvist, H. and Wiklund, U., Mapping of mechanical properties of WC–Co using nanoindentation. *Tribol. Lett.*, 2000, **8**, 147–152.
13. Park, K., Mishra, S., Lewis, G., Losby, J., Fan, Z. and Park, J. B., Quasi-static and dynamic nanoindentation studies on highly cross-linked ultra-high-molecular-weight polyethylene. *Biomaterials*, 2004, **25**, 2427–2436.
14. Kumar, R. R. and Wang, M., Functionally graded bioactive coatings of hydroxyapatite/titanium oxide composite system. *Mater. Lett.*, 2002, **55**, 133–137.
15. Oliver, W. C. and Pharr, G. M., An improved technique for determining hardness and elastic modulus using load and displacement sensing indentation experiments. *J. Mater. Res.*, 1992, **7**, 1564–1583.
16. Asif, S. A. S., Wahl, K. J. and Colton, R. J., Nanoindentation and contact stiffness measurement using force modulation with a capacitive load-displacement transducer. *Rev. Sci. Instrum.*, 1999, **70**, 2408–2413.
17. Asif, S. A. S., Wahl, K. J., Colton, R. J. and Warren, O. L., Quantitative imaging of nanoscale mechanical properties using hybrid nanoindentation and force modulation. *J. Appl. Phys.*, 2001, **90**, 1192–1200.
18. Balooch, G., Marshall, G. W., Marshall, S. J., Warren, O. L., Asif, S. A. S. and Balooch, M., Evaluation of a new modulus mapping technique to investigate microstructural features of human teeth. *J. Biomech.*, 2004, **37**, 1223–1232.
19. Olek, M., Kempa, K., Jurga, S. and Giersig, M., Nanomechanical properties of silica-coated multiwall carbon nanotubes–poly(methyl methacrylate) composites. *Langmuir*, 2005, **21**, 3146–3152.
20. Ngan, A. H. W., Wang, H. T., Tang, B. and Sze, K. Y., Correcting power-law viscoelastic effects in elastic modulus measurement using depth-sensing indentation. *Int. J. Solids Struct.*, 2005, **42**, 1831–1846.
21. Gregory, J. R. and Spearing, S. M., Nanoindentation of neat and in situ polymers in polymer–matrix composites. *Compos. Sci. Technol.*, 2005, **65**, 595–607.
22. Kumar, R. R. and Wang, M., Modulus and hardness evaluations of sintered bioceramic powders and functionally graded bioactive composites by nanoindentation technique. *Mater. Sci. Eng. A*, 2002, **338**, 230–236.
23. Shikinami, Y. and Okuno, M., Bioresorbable devices made of forged composites of hydroxyapatite (HA) particles and poly-L-lactide (PLLA). Part I. Basic characteristics. *Biomaterials*, 1999, **20**, 859–877.
24. Wright-Charlesworth, D. D., Miller, D. M., Miskioglu, I. and King, J. A., Nanoindentation of injection molded PLA and self-reinforced composite PLA after in vitro conditioning for three months. *J. Biomed. Mater. Res.*, 2005, **74**, 388–396.
25. Sharp, J. S. and Jones, R. A. L., Swelling-induced morphology in ultrathin supported films of poly(D,L-lactide). *Phys. Rev. E*, 2002, **660**, 389–397.
26. Wang, M., Yue, C. Y. and Chua, B., Production and evaluation of hydroxyapatite reinforced polysulfone for tissue replacement. *J. Mater. Sci.: Mater. Med.*, 2001, **12**, 821–826.
27. Zhang, R. and Ma, P. X., Porous poly(L-lactic acid)/apatite composites created by biomimetic process. *J. Biomed. Mater. Res.*, 1999, **45**, 285–293.